XLVI CILAMCE
VITÓRIA - ES - BRAZIL - 2025
XLVI IBERO-LATIN AMERICAN CONGRESS ON COMPUTATIONAL METHODS IN ENGENEERING

Analysis of incompressible flows with free surfaces and slip walls using a position-based PFEM approach

Thiago R. Carvalho[1], Giovane Avancini[2], Rodolfo A. K. Sanches[1]

[1]*São Carlos School of Engineering (EESC), University of São Paulo (USP)*
Av. Trabalhador São carlense 400, 13566-590, São Carlos - SP, Brazil
thiagorc7@usp.br, rodolfo.sanches@usp.br
[2]*Dept. of Structural Engineering, Faculty of Civil Engineering, State University of Campinas (Unicamp)*
R. Saturnino de Brito 224, 13083-889, Campinas - SP, Brazil
giovanea@unicamp.br

Abstract. Moving-boundary incompressible flows with topological changes present major challenges for numerical simulation. The Particle Finite Element Method (PFEM) has proven to be a robust framework for such problems, especially due to its ability to handle large domain distortions and free surfaces. In the PFEM approach, the Delaunay triangulation is applied over a cloud of particles at each time step, and the alpha-shape method is employed to remove non-physical elements and define the domain boundaries. However, when wall particles are allowed to slide tangentially along slip boundaries, the resulting mesh may become distorted, leading to the removal of elements at the boundary by the alpha-shape procedure and, ultimately, causing artificial leakage and loss of physical boundary representation. This work proposes a particle-position-based strategy to incorporate slip-wall conditions into PFEM simulations while preserving mesh integrity. The method relies on a nodal repositioning technique that restores the original geometry of the slip boundary after particle motion, ensuring that wall elements are retained during remeshing. This approach enables the accurate and robust simulation of flows with free surfaces and sliding walls without sacrificing the advantages of the position-based PFEM formulation. The proposed methodology also maintains compatibility with structural systems, allowing the potential for straightforward monolithic coupling in fluid–structure interaction problems. Numerical examples demonstrate the accuracy and robustness of the formulation in preserving slip-wall behavior and domain integrity, even in highly dynamic flow scenarios.

Keywords: PFEM, Position-based, Slip boundaries, Incompressible flows.

1 Introduction

Numerical analysis of fluid flow has numerous applications in engineering, but yet there is no general and efficient computational method available that can simulate all the different situations. In this context, the development of alternative numerical formulations, such as the Particle Finite Element Method (PFEM), has emerged as advantageous in certain contexts.

The PFEM was proposed by Idelsohn et al. [1] to combine particle and mesh concepts to treat problems with indefinite distortions and topological changes in the finite element mesh that cannot be accommodated by the deformation of the fluid mesh, such as free-surface flows. Originally, this method was developed using a updated Lagrangian description of the fluid's governing equations and an approach based on classical velocity-pressure finite element approximation.

This method has been applied in several contexts, such as to simulate incompressible flows with free surfaces, breaking waves, non-Newtonian free surface flows, fresh concrete flow, and interaction between structures and free surface flows (see e.g.Aubry et al. [2], Idelsohn et al. [3, 4], Cerquagliaa et al. [5], Franci [6], Cerquaglia et al. [7], Larese [8], Rizzieri et al. [9] and Fu et al. [10]

Alternatively, Avancini et al. [11] proposed a particle-position based PFEM approach that uses a partially updated Lagrangian description, which was inspired by the position-based approach developed in the nonlinear solid mechanics context [12–14]. This new PFEM approach has been successfully applied to the analysis of 2D and 3D free-surface flows and fluid-structure interaction (FSI) problems with free-surface flows [11, 15], FSI with structural contact [16], two-dimensional bi-phase [17] and multiphase [18] flows, as well as to the analysis of

non-Newtonian fresh concrete flow [19].

In addition to the advantages of traditional PFEM, the position-based approach offers a straight-forward and easy way to build a monolithic FSI solver [15, 16, 20]. This approach also provides better consistency for in representing the deformed geometry, especially in FSI problems with large displacements. The velocity-based PFEM requires an additional step to calculate numerically the current particle positions from the velocities, introducing a new source of numerical error, whereas in the positional approach, the current geometry is directly determined by the numerical system's solution.

Although robust, both PFEM approaches – positional and traditional – have limitations for application to open-domain flows with inflow and/or outflow boundaries, and also to problems with slip wall boundaries. The slip boundary condition poses a challenge because, upon releasing the tangential motion component of the particles on the walls, the material motion can distort the elements with sides at walls, consequently resulting in its removal, either by the α-shape criterion or other mesh quality control criterion, degenerating the boundary and, possibly, leading to leakage.

In this context, this work proposes a technique to introduce slip-wall boundary conditions in the particle-position based PFEM. This technique is implemented and successfully applied to two-dimensional flows. The use of slip-walls allows the PFEM to be applied to a broader range of problems and is useful when it is desired to neglect minor boundary layer effects.

2 Governing equations for incompressible Newtonian flows in a partially updated Lagrangian description

The partially updated Lagrangian description of the linear momentum equation is given by (see [11]):

$$\rho\ddot{\mathbf{x}}_{n+1} - \nabla_n \cdot (\mathbf{S} \cdot \mathbf{F}_n^T) - \mathbf{b}_n = \mathbf{0}, \tag{1}$$

where ρ refers to density; $\ddot{\mathbf{x}}_{n+1}$ refers to current acceleration; $\mathbf{F}_n$ refers to the deformation gradient from the reference configuration Ω_n to the current configuration Ω_{n+1}; $\mathbf{b}_n$ refers to the body forces; and $\mathbf{S}$ is the second Piola-Kirchhoff stress tensor defined with respect to the reference configuration.

Note that the reference configuration for the fluid is taken as the last known equilibrium configuration Ω_n (clculated at instant t_n).

The mass conservation can be expressed locally as:

$$\rho_{n+1} J = \rho_n, \tag{2}$$

where J denotes the scalar Jacobian of the deformation from the reference to the current configuration (determinant of $\mathbf{F}_n$); ρ_{n+1} is the current density and ρ_n is the reference density.

Considering incompressibility, ρ is constant and the mass conservation resumes to $J - 1 = 0$.

2.1 Constitutive model

The constitutive relationship for incompressible Newtonian flows in terms of second Piola-Kirchhoff stress tensor ($\mathbf{S}$) and Green strain rate tensor ($\dot{\mathbf{E}}$) may be written as (see [21]):

$$\mathbf{S} = \mathfrak{D}_n : \dot{\mathbf{E}} - pJ\mathbf{C}^{-1}. \tag{3}$$

where p denotes the pressure; $\mathbf{C}$ is the right Cauchy-Green stretch tensor from Ω_n to Ω_{n+1} and $\mathfrak{D}_n$ is the fourth order constitutive tensor given by:

$$(\mathfrak{D}_n)_{ijkl} = J_n (F_n^{-1})_{ia} (F_n^{-1})_{jb} (F_n^{-1})_{kc} (F_n^{-1})_{ld} (\mathfrak{D}_{n+1})_{abcd}, \tag{4}$$

$\mathfrak{D}_n$ is the constitutive tensor in the reference configuration, $(\mathfrak{D}_{n+1})_{abcd} = \mu\left(\delta_{ac}\delta_{bd} + \delta_{ad}\delta_{bc}\right)$ is the constitutive tensor in the current configuration, with μ being the dynamic viscosity.

3 Position-based PFEM for incompressible flows

The fundamental idea of PFEM is to represent the fluid domain by a cloud of particles, with a finite element mesh being built, taking the particles as nodes, to solve the motion equations and update the particle positions. At the end of each time step, the mesh is erased and reconstructed for the next step solution. The process of remeshing is associated with a geometric criterion to define the fluid subdomains and boundaries [1, 2, 4, 11].

3.1 Finite element formulation for one finite step

A weak form of the governing equations presented in section **??** suitable for finite element discretization can be obtained by applying energy conservation principle as presented by Avancini and Sanches [21], taking nodal (particle) current positions and pressure as variational parameters.

Considering energy conservation regarding variation of position combined with the finite element technique, it results the semi-discrete weak form of the momentum equation:

$$\int_{\Omega_n} \rho \boldsymbol{\phi}_a \cdot \ddot{\mathbf{x}}^h_{n+1} d\Omega_n + \int_{\Omega_n} \dot{\mathbf{E}}^h : \mathfrak{D}^h_n : \frac{\partial \mathbf{E}^h_n}{\partial (\mathbf{x}_{n+1})_a} d\Omega_n - \int_{\Omega_n} p^h \frac{\partial J^h_n}{\partial (\mathbf{x}_{n+1})_a} d\Omega_n - \int_{\Omega_n} \boldsymbol{\phi}_a \cdot \mathbf{b}_n d\Omega_n - \int_{\Gamma_n} \boldsymbol{\phi}_a \cdot \mathbf{f}^{sup}_n d\Gamma_n = \mathbf{0}_a, \tag{5}$$

where $\boldsymbol{\phi}_a$ denotes the position shape function associated to node a; $\ddot{\mathbf{x}}^h_{n+1}$ is the current acceleration; $\dot{\mathbf{E}}^h$ is the Green's strain rate tensor; $\mathbf{E}^h$ refers to Green's strain tensor; $(\mathbf{x}_{n+1})_a$ is the current position of node a; $\mathbf{f}^{sup}_n$ refers to surface tractions; p^h denotes the pressure.

PFEM requires pressure and positions to be interpolated by linear shape functions; however, it can lead to spurious pressure fields and numerical instabilities as a result of the violation of the inf-sup conditions for incompressible flows [22]. Thus, the application of energy conservation regarding pressure variation within the finite element procedure needs to be followed by the introduction of a pressure stabilizing technique. Following Avancini et al. [11], we use the Petrov-Galerking Pressure Stabilization (PSPG), introduced by Tezduyar [23], leading to the stabilized weak form of the incompressibility condition:

$$-\int_{\Omega_n} \phi_a (J^h_n - 1) d\Omega_n + \int_{\Omega_n} \tau_{PSPG} \frac{1}{\rho} [(\mathbf{F}^h_n)^{-T} \cdot \nabla_n \phi_a] d\Omega_n \cdot [\rho \ddot{\mathbf{x}}^h_{n+1} - \nabla_n \cdot (\mathbf{S}^h \cdot (\mathbf{F}^h_n)^T) - \mathbf{b}_n] d\Omega_n = 0_a, \tag{6}$$

where τ_{PSPG} refers to the stabilizing parameter (see Avancini et al. [11]) and ϕ_a is the pressure shape function associated to node a.

To get the fully discrete equations, we use the time-marching α-generalized method, leading to a nonlinear system that is solved by the Newton-Raphson technique, as shown in Avancini et al. [11].

3.2 Particle Finite Element Method

In the PFEM, a particle is defined as a material point that carries the physical properties of the fluid to which it belongs, such as density and viscosity, as well as the problem variables such as pressure and velocity or position.

A new continuous, piecewise-differentiable mesh is generated using the same techniques as the traditional FEM. This mesh provides the shape functions that allow spatial discretization of the Navier-Stokes equations, and consequently, allows the evaluation of the interaction forces between particles and the solution of the motion equation. This mesh is erased and a new is generated for each new particle configuration, or when the quality of the current mesh is compromised, maintaining the nodal values (of the particles) from previous mesh. To reconstruct the mesh without compromising the domain definition, the Delaunay Triangulation method is used along with the α-shape method to identify the boundaries.

However, the fact that Newtonian fluids cannot statically withstand shear stresses, as can be seen in Fox et al. [24], means that some particles can come very close to each other, resulting in poor mesh quality, with highly distorted or very small elements. In this sense, particle relocation techniques can be employed before the new mesh is generated, with the nodal values interpolated to the position where they are relocated using the shape functions of the last discretization, thus ensuring mesh quality.

It should be noted, however, that when the connectivity between nodes is altered by replacing the mesh, the solution calculated in the previous time step may no longer satisfy the equilibrium and incompressibility conditions in the new mesh, even in weak sense. This perturbation is small and decreases with the refinement of the spatial discretization (see Avancini et al. [11]).

Adaptive re-mesh to treat slip-walls

The application of slip conditions can be easily applied in both, Eulerian and Lagrangian FEM descriptions by releasing the tangential motion component for the fluid at slip walls. In the PFEM, the ghost particle process makes it simple to impose adherent wall boundary conditions. However, this process makes it difficult to allow particles to slide over the walls, as the representation of the walls by the ghost particles gets distorted as particles move apart, specially for particles close to other boundaries, which can excessively distort the elements associated with these boundary particles. To avoid numerical problems, this distorted elements will be removed during α-shape application, creating an opening in the wall.

Thus, the fundamental idea of the technique proposed here is to allow controlled sliding by relocating the slip-wall particles to their initial position after each time step, with their velocity and pressure values being replaced by the values interpolated at the closest point to their original position within the deformed mesh boundary before relocation. Notice that the velocity, pressure, and acceleration values may be different from the initial ones; therefore, it is also necessary to interpolate these values at the initial positions after relocation.

Thus, whenever mesh reconstruction is triggered, the code automatically identifies the ghost particles of the slip-walls and recovers the initial geometry of the walls, from the relocation to their initial positions.

4 Numerical examples

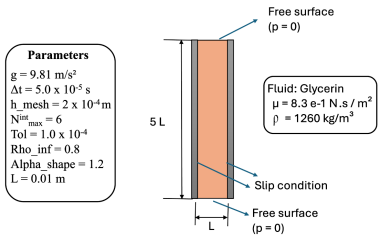
In this section, we present numerical examples that are typically solved with Eulerian approaches to verify the proposed formulation.

4.1 Flow with slip-walls and free surface

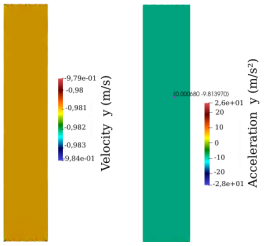
This example aims to verify the proposed slip-wall treatment in the context of a free-surface flow.

The problem consists of a portion of glycerin flowing inside a long tube with slip-walls. The fluid has dimensions [L x 5L], where L = 0.01 m, as shown in Figure 2(a). At upper and lower faces, we assume null traction boundary condition so that the fluid is under the action of gravity only, what should result in rigid body motion for the fluid domain. The movement of this set of fluid particles is monitored inside the tube to verify the application of the sliding conditions, according to the methodology described in 3.2.

Glycerin is simulated with the physical properties $\mu = 0.83\,\mathrm{N\,s\,m^{-2}}$ and $\rho = 1260\,\mathrm{kg\,m^{-3}}$. The gravity acceleration is considere $g = 9.81\,\mathrm{m\,s^{-2}}$ and the problem is initially discretized with linear approximation triangular elements of characteristic length h =0.0002 m. The adopted time step is $\Delta t = 0.000\,05\,\mathrm{s}$ and the spectral radius for the generalized-α integrator is $\rho_\infty = 0.8$.



((a)) Geometry and properties.



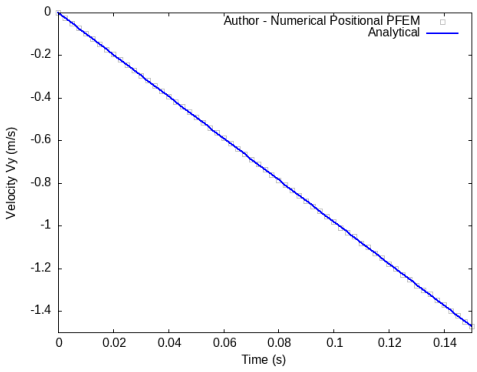
((b)) Velocity and Acceleration fields at specific instants.

Figure 1. Flow with slip-walls and free surface: Geometry and flow characteristics (a) and fields snapshots (b).

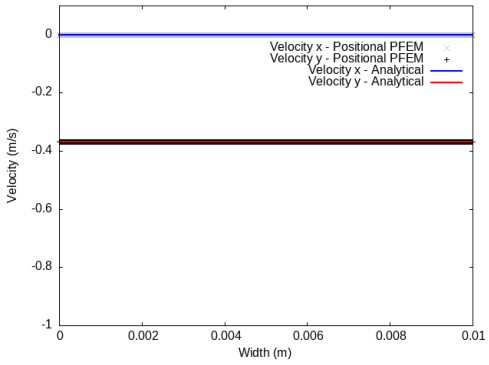
Figure 1(b) shows the obtained fields of vertical velocity component at instant $t = 0.10\,\mathrm{s}$ and vertical acceleration at $t = 0.075\,\mathrm{s}$. The fields present the expected values for the analytical solution of this problem. The fields also highlight the spatial smoothness of the fields and their temporal stability.

Finally, Figure 2 shows the information extracted along the cross-section at 0.01 m above the bottom of the fluid domain compared with analytical predictions. Figure 2(a) compares the vertical velocity over time with the

analytical solution, while Figure 2(b) compares the distribution of velocity components along the width with the analytical values. One can see very good agreement of numerical solutions to the expected analytical solutions.



((a)) Longitudinal velocity v_y over time.



((b)) Velocity profiles v_x and v_y.

Figure 2. Flow with slip-walls and free surface: Velocity profiles.

4.2 Flow over a cylinder with vortex shedding

This is one of the classical examples used to verify usual CFD codes (using Eulerian description) and consists of a cylinder subjected to incompressible flow producing von Kármán vortex wake. In the context of PFEM, in addition to the challenges of representing spatially fixed inlet and outlet boundaries, the vortex wake presents a challenge that tests the reconstruction technique and mesh quality control.

The initial geometry and finite element mesh, as well as analysis parameters and physical properties are presented in Figure 3. The left side wall represents an inlet boundary where the fluid enters at constant velocity $v_x = 1.0$ m/s, so that new particles enter the domain along the solution process with this velocity along the solution. The right side wall is considered a flow outlet, where particles are removed from the analysis as they cross this wall. The upper and lower walls are slip impermeable walls. A generic fluid with $\rho = 1\,\mathrm{kg\,m^{-3}}$ and dynamic viscosity of $\mu = 0.01\,\mathrm{N\,s\,m^{-2}}$ is used, resulting a Reynolds $Re = 100$ with reference to the cylinder diameter. The initial finite element discretization has triangular linear finite elements with characteristic length h =0.2 m.

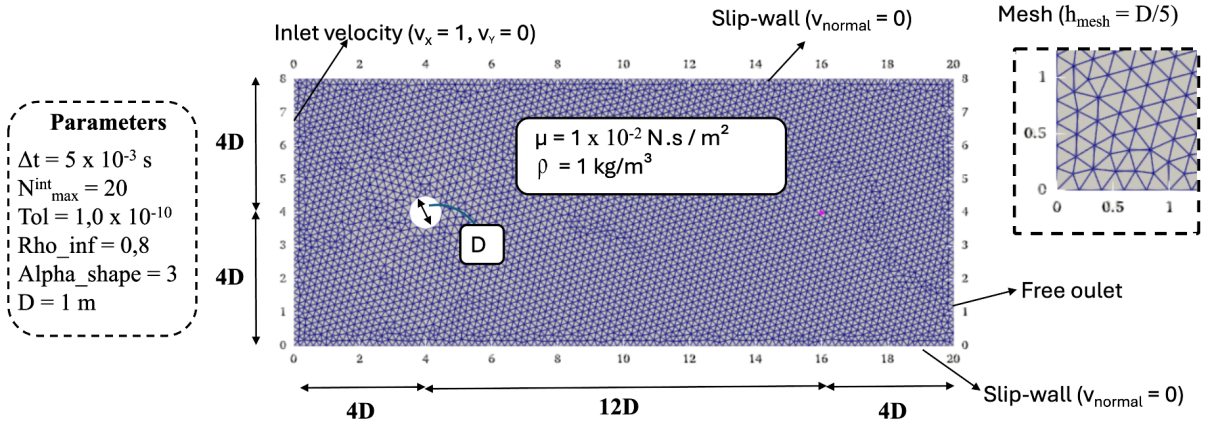
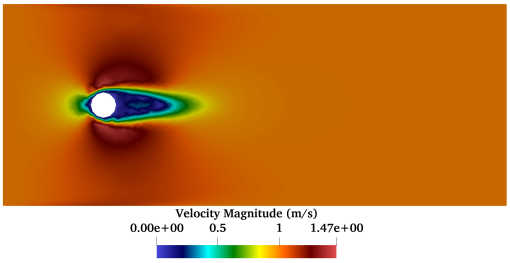
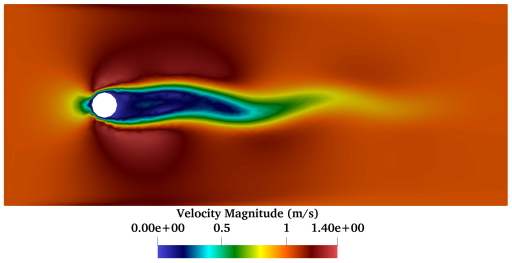


Figure 3. Flow around a cylinder: geometry, boundary conditions and initial mesh.

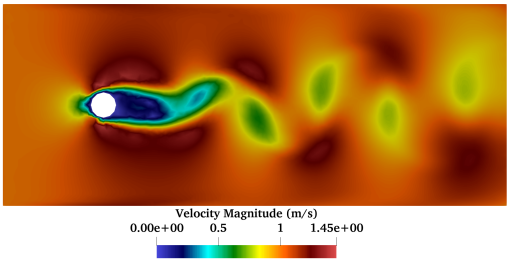
The velocity distribution (absolute values) is presented for different instants in Figure 4, where it is possible to observe both the beginning of vortex shedding and the fully developed wake. Figure 4(d) illustrates the result of the velocity field for the average instant of time, obtained by Fernandes [25]. These results are consistent with the expected solution, giving qualitative evidence that the proposed formulation is able to deal not only with the free-surface flows where PFEM is typically applied with efficiency, but also with other complex problems where Eulerian methods are considered more efficient.



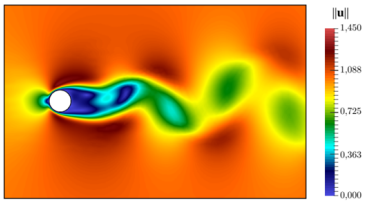
((a)) t = 5.



((b)) t = 15.



((c)) t = 60.



((d)) t = average time instant [25].

Figure 4. Flow around a cylinder: Velocity magnitude snapshots.

5 Conclusions

In this paper we introduced a methodology to consider slip-walls boundary conditions in the particle-position-based PFEM formulation to incompressible Newtonian fluids. This methodology was implementation and tested using a simple numerical example of a flow with slip-walls whose results were compared with analytical data, and then applied to the simulation of viscous flow over a cylinder with vortex shedding, showing good behavior. Further investigation is needed to assess the robustness and accuracy of the methodology in other examples. For future works, authors are interested in expanding the implementations to generalized open domain conditions in 3D problems, as well as to the study of fluid-structure interaction with slip condition at the fluid-structure interface.

Acknowledgements. The authors gratefully acknowledge the financial support provided by the Coordination for the Improvement of Higher Education Personnel (CAPES) – Finance Code 001, the National Council for Scientific and Technological Development (CNPq) – grant 314045/2023-6, and the São Paulo Research Foundation (FAPESP) – project 2024/05554-9. The authors are also grateful for the infrastructure of the Department of Structures SET/EESC and the University of São Paulo.

Authorship statement. The authors hereby confirm that they are the sole liable persons responsible for the authorship of this work, and that all material that has been herein included as part of the present paper is either the property (and authorship) of the authors, or has the permission of the owners to be included here.

References

[1] S. R. Idelsohn, E. Onate, and F. D. Pin. The particle finite element method: a powerful tool to solve incompressible flows with free-surfaces and breaking waves. *International journal for numerical methods in engineering*, vol. 61, n. 7, pp. 964–989, 2004.

[2] R. Aubry, S. Idelsohn, and E. Onate. Fractional step-like schemes for free surface problems with thermal coupling using the lagrangian pfem. *Computational Mechanics*, vol. 38, n. 4-5, pp. 294–309, 2006.

[3] S. Idelsohn, J. Marti, P. Becker, and E. Oñate. Analysis of multifluid flows with large time steps using the particlefinite element method. *Inter. J. Num. Meth. Fluids*, vol. 75, pp. 621–644, 2014.

[4] S. Idelsohn, J. Marti, A. Souto-Iglesias, and E. Onate. Interaction between an elastic structure and free-surface flows: experimental versus numerical comparisons using the pfem. *Computational Mechanics*, vol. 43, n. 1, pp.

125–132, 2008.
[5] M. Cerquagliaa, D. Thomasa, R. Bomana, V. Terrapona, and J.-P. Ponthota. A fully partitioned lagrangian framework for fsi problems characterized by free surfaces, large solid deformations and displacements, and strong added-mass effects. *omput. Methods Appl. Mech. Engrg.*, vol. 348, n. 409-442, 2019.
[6] A. Franci. *Unified Lagrangian formulation for fluid and solid mechanics, fluid-structure interaction and coupled thermal problems using the PFEM*. Springer, 2016.
[7] M. L. Cerquaglia, G. Deliége, R. Boman, L. Papeleux, and J. Ponthot. The particle finite element method for the numerical simulation of bird strike. *International journal of impact engineering*, vol. 109, pp. 1–13, 2017.
[8] A. Larese. A lagrangian pfem approach for non-newtonian viscoplastic materials. *Revista Inter. de Mét. Num. para Cál. y Diseño en Ingeniería*, pp. 307–317, 2017.
[9] G. Rizzieri, L. Ferrara, and M. Cremonesi. Numerical simulation of the extrusion and layer deposition processes in 3d concrete printing with the particle finite element method. *Comp. Mech.*, vol. 73, pp. 277–295, 2024.
[10] C. Fu, M. Cremonesi, and U. Perego. A hybrid lagrangian–eulerian particle finite element method for free-surface and fluid–structure interaction problems. *Int. J. Numer. Met. Eng.*, 2023.
[11] G. Avancini, A. Franci, S. Idelsohn, and R. Sanches. A particle-position-based finite element formulation for free-surface flows with topological changes. *Computer Methods in Applied Mechanics and Engineering*, vol. 429, 2024.
[12] H. B. Coda. *Análise não linear geométrica de sólidos e estruturas: Uma formulação posicional baseada no MEF*. PhD thesis, SET-EESC-USP, São Carlos, São Paulo, Brasil, 2003.
[13] H. B. Coda and R. R. Paccola. An alternative positional fem formulation for geometrically non-linear analysis of shells: curved triangular isoparametric elements. *Computational Mechanics*, vol. 40, n. 1, pp. 185–200, 2007.
[14] H. B. Coda. *O Método dos elementos finitos posicional: sólidos e estruturas - não linearidade geométrica e dinâmica*. EESC/USP, São Carlos, 2018.
[15] G. Avancini. *Formulação unificada para análise tridimensional de interação fluido-estrutura com escoamento de superfície livre: Uma abordagem Lagrangiana baseada em posições*. PhD thesis, Escola de Engenharia de São Carlos, Universidade de São Paulo, São Carlos, 2023.
[16] D. H. F. R. Moreira. Análise numérica bidimensional de interação fluido-estrutura com contato estrutural. Master's thesis, Escola de Engenharia de São Carlos, Universidade de São Paulo, São Carlos, 2021.
[17] T. R. Carvalho, G. Avancini, and R. A. K. Sanches. Analysis of two-phase flows using position-based pfem formulation. In *In XLV Iberian-Latin American Congress On Computational Methods In Engineering*, 2024.
[18] T. R. Carvalho, G. Avancini, and R. A. K. Sanches. Two-dimensional numerical analysis of multiphase flows using a pfem particle position-based formulation. In *8th Multiphase Flows Journey*, 2025.
[19] L. F. H. Teodoro, G. Avancini, and R. A. K. Sanches. A position-based pfem formulation for free-surface non-newtonian flows with application to fresh concrete. In *Ibero-Latin American Congress on Computational Methods in Engineering (CILAMCE)*, 2024.
[20] T. R. Carvalho. Análise numérica de interação fluido-estrutura com escoamentos multifásicos: uma abordagem monolítica em descrição lagrangiana. Master's thesis, Escola de Engenharia de São Carlos, Universidade de São Paulo, São Carlos, 2025.
[21] G. Avancini and R. A. K. Sanches. A total lagrangian position-based finite element formulation for free-surface incompressible flows. *Finite Elements in Analysis and Design*, vol. 169, 2020.
[22] K.-J. Bathe, D. Hendriana, F. Brezzi, and G. Sangalli. Inf–sup testing of upwind methods. *International Journal for Numerical Methods in Engineering*, vol. 48, n. 5, pp. 745–760, 2000.
[23] T. E. Tezduyar. Stabilized finite element formulations for incompressible flow computations. *Advances in applied mechanics*, vol. 28, pp. 1–44, 1991.
[24] R. W. Fox, A. T. McDonald, P. J. Pritchard, and J. W. Mitchell. *Introdução à Mecânica dos Fluidos*. LTC - Grupo GEN, Rio de Janeiro - RJ, 9 edition, 2020.
[25] J. W. D. Fernandes. *Técnica de superposição de modelos estabilizada para análise de interação fluido-estrutura*. Tese (doutorado em engenharia de estruturas) – departamento de engenharia de estruturas, escola de engenharia de são carlos, Universidade de São Paulo, São Carlos, 2020.